Complete Continuous Delay Regions, Quantized Passive Memory, and Pick Tomography for Quantum Networks

Lluis Eriksson

10 August 2026

Abstract

Lower bounds do not determine which resource profiles are physically attainable. We close the continuous inverse problem for passive subspace transport. Let two rank-k subspaces in $\mathbb{C}^N$, $N \geq 2k$, have ordered canonical angles β, and let $q_j = \int \lambda_j(Q(t))\,\mathrm{d}t$ be the integrated leading eigenvalues of a positive generator $Q = -\mathrm{i}S^*\dot{S}$. We prove the exact equivalence

$$q \text{ is attainable} \quad \Longleftrightarrow \quad 2\beta \prec_w q.$$

Every feasible profile has a compiler using at most $k+1$ mutually commuting, positive generators of rank at most k whose ordered top spectrum is constant in time; the Carathéodory count is generically sharp within this signed-orbit compiler class. Analytic rationality adds a different, integer-valued resource. For two boundary frequencies, the least McMillan degree of an inner matrix that sends a fixed input subspace to two prescribed output subspaces is exactly the number of nonzero canonical angles. Thus arbitrarily small full-rank motion has vanishing continuous action but a fixed k-state memory cost. We give a fail-closed finite-error certificate for both resources from noisy projectors.

At multiple frequencies, we show that Wigner–Smith delay is only the block diagonal of a boundary de Branges–Rovnyak Pick matrix. This matrix is positive, has rank at most the McMillan degree, and is the Gram matrix of the internal states excited by the measured frequencies and channels. Its spectrum yields robust degree certificates and unavoidable model-reduction tails. An exact scalar example has identical proper delays at two frequencies for degree one and degree two, while the corresponding Pick ranks are one and two. A transfer-matrix corollary identifies Euclidean correlators as Fourier coefficients of a proper-delay spectrum and a spectral gap as a zero-frequency delay cap; it is a dictionary, not a mass-gap proof. Deterministic code reconstructs the compilers, tests 2,240 randomized theorem interfaces, checks the strict separation, and independently replays the certificate.

Keywords: passive quantum network; Wigner–Smith delay; weak majorization; McMillan degree; rational inner function; Pick matrix; de Branges–Rovnyak kernel; subspace transport; mass gap.

1 Two resources hidden in one routing event

The preceding papers in this programme progressed from finite-sample spectral exclusion and noncommuting architectural separation to passive reservoir filters, topological memory, robust routing and a complete Ky Fan speed-limit hierarchy [7, 8, 5, 10, 6, 11]. The sixth paper proved that if a rank-k subspace moves through canonical angles $\beta_1 \geq \cdots \geq \beta_k$, then its integrated proper-delay profile q must satisfy

$$2\beta \prec_w q, \qquad 2\sum_{j=1}^{r} \beta_j \leq \sum_{j=1}^{r} q_j, \quad r = 1, \ldots, k. \tag{1}$$

Every symmetric-gauge minimum follows from this Lorenz-curve inequality. What remained open was whether (1) is merely an obstruction or the complete feasible region.

We answer that question and then expose a second resource that no continuous speed limit can see. A rational inner transfer matrix has an integer McMillan degree. We prove that the least degree needed to create a two-point subspace rotation is the support size of the canonical-angle vector, not its norm. Continuous action prices the amplitude of motion; rational degree prices how many independent directions move at all.

The multi-frequency completion is a positive kernel. For a rational inner S define

$$K_S(z,w) = \frac{I - S(z)S(w)^*}{1 - z\bar{w}}. \tag{2}$$

At a boundary point its diagonal is a unitary conjugate of Wigner–Smith delay. Off the diagonal it records overlaps between frequency-excited internal states. Those cross terms distinguish devices whose local delay spectra agree.

The ingredients are classical and we keep the priority boundary explicit. Weak majorization and signed permutahedra belong to majorization theory [15]; Grassmann metrics are due to Qiu, Zhang and Li [18], with a recent projector-based treatment of shortest Grassmann paths given by Huang [14]; spectral-spread block inequalities are due to Massey, Stojanoff and Zárate [16]; boundary Schur interpolation and de Branges–Rovnyak spaces are established theories [4, 3]; and minimal passive quantum realizations are classical system theory [17, 13]. General minimum-degree rational matrix interpolation predates this work [2], and a recent realization theory computes McMillan degree from positive choice sequences [12]. Our contribution is the exact attainable delay region and compiler, the sharp two-subspace degree quantization, their joint robust certificate, and the operational Pick–Wigner–Smith memory tomography built from finite scattering data.

Priority audit and precise scope. The Grassmann literature cited above determines canonical-angle metrics and shortest paths, but does not prescribe a positive unitary lift with a fixed integrated leading-eigenvalue profile. The first result below adds exactly that constrained inverse synthesis. Classical tangential interpolation is substantially more general than our two-node setting; the second result should therefore be read as an explicit exact specialization to subspace-valued boundary data, not as a new general interpolation theory. In the sources located in a targeted audit through 10 August 2026, we did not find the formula “minimum degree = number of nonzero canonical angles” stated for this quotient problem. Finally, positivity and finite-rank factorization of the de Branges–Rovnyak kernel are classical; the contribution of the last part is its operational assembly from Wigner–Smith data, the strict local-delay blindness example, and the fail-closed noisy rank certificate.

2 Setup and the necessary Lorenz law

Let $\mathcal{X}, \mathcal{Y} \subset \mathbb{C}^N$ have rank k, with $N \geq 2k$. Their ordered canonical angles are $\beta_1 \geq \cdots \geq \beta_k \in [0, \pi/2]$. Let $S : [0, \Delta] \to U(N)$ be absolutely continuous, $S(0)\mathcal{X} = \mathcal{X}$ and $S(\Delta)\mathcal{X} = \mathcal{Y}$, and put

$$Q(t) = -\mathrm{i}S(t)^*\dot{S}(t). \tag{3}$$

We call the path passive-monotone when $Q(t) \succeq 0$ almost everywhere. Its integrated leading-delay profile is

$$q_j = \int_0^\Delta \lambda_j(Q(t))\,\mathrm{d}t, \qquad q_1 \geq \cdots \geq q_k \geq 0. \tag{4}$$

The time-dependent spectral-spread theorem of [11], obtained by composing a Grassmann path-length law with the block inequality of [16], gives (1). This is the only necessity input used below.

3 The complete delay region

Write $\mathfrak{B}_k$ for the group of signed permutation matrices. A standard orbit-polytope form of weak majorization says, for nonnegative decreasing $x, q \in \mathbb{R}^k$,

$$x \prec_w q \iff x \in \mathrm{conv}\{Rq : R \in \mathfrak{B}_k\}. \tag{5}$$

The signs, which are irrelevant to symmetric norms, acquire a physical meaning here: they reverse motion in a principal plane while preserving positive proper delay.

Theorem 3.1 (Complete positive-delay region)**.** *Let $N \geq 2k$ and let $q \in \mathbb{R}^k$ be nonnegative and decreasing. There exists an absolutely continuous path transporting $\mathcal{X}$ to $\mathcal{Y}$, with $Q(t) \succeq 0$ and integrated profile* (4)*, if and only if*

$$2\beta \prec_w q. \tag{6}$$

Whenever (6) *holds, there is such a path with all of the following properties:*

1. *at most $k+1$ piecewise-constant segments;*
2. $\operatorname{rank} Q(t) \leq k$*;*
3. $(\lambda_1(Q(t)), \dots, \lambda_k(Q(t))) = q/\Delta$ *almost everywhere;*
4. *all segment generators commute.*

The same equivalence holds if q denotes the integrated first k spectral spreads of an arbitrary Hermitian generator.

Proof. Necessity is (1). For sufficiency, apply (5) and Carathéodory's theorem in $\mathbb{R}^k$: there are $m \leq k+1$, weights $t_s \geq 0$ summing to one and $R_s \in \mathfrak{B}_k$ such that

$$2\beta = \sum_{s=1}^{m} t_s R_s q. \tag{7}$$

Choose principal pairs e_j, f_j so that

$$\mathcal{X} = \operatorname{span}\{e_j\}_{j=1}^k, \qquad \mathcal{Y} = \operatorname{span}\{\cos\beta_j e_j - \sin\beta_j f_j\}_{j=1}^k.$$

Write $(R_s q)_j = \varepsilon_{s,j} q_{\pi_s(j)}$. On a segment of duration $t_s\Delta$, define, in the plane $\operatorname{span}\{e_j, f_j\}$,

$$Q_{s,j} = \frac{q_{\pi_s(j)}}{2\Delta} \begin{bmatrix} 1 & -\mathrm{i}\varepsilon_{s,j} \\ \mathrm{i}\varepsilon_{s,j} & 1 \end{bmatrix}. \tag{8}$$

Each block is positive with eigenvalues $q_{\pi_s(j)}/\Delta$ and zero. Thus $Q_s = \bigoplus_j Q_{s,j}$ has rank at most k and ordered top spectrum q/Δ.

For a fixed plane, the two possible normalized blocks in (8) are complementary rank-one projections, so they commute; blocks in distinct planes also commute. The signed rotation accumulated in plane j is

$$\frac{1}{2} \sum_s t_s \varepsilon_{s,j} q_{\pi_s(j)} = \beta_j$$

by (7). Hence the endpoint is $\mathcal{Y}$ and the integrated ordered spectrum is exactly q. The constructed positive rank-k generator has $N-k$ zero eigenvalues, so its first k spectral spreads also equal its leading eigenvalues. Unitary conjugation places the construction in arbitrary principal frames. □

Proposition 3.2 (Sharpness within signed-orbit compilation)**.** *If $q_1 > \cdots > q_k > 0$, then almost every point in the signed permutahedron $\operatorname{conv}(\mathfrak{B}_k q)$ requires $k+1$ vertices in a convex representation. Consequently, the $k+1$ segment count in the signed-orbit construction of Theorem 3.1 cannot be lowered uniformly within that compiler class.*

Proof. The signed permutahedron is full-dimensional. The points representable by at most k vertices form a finite union of simplices of dimension at most $k-1$, hence have Lebesgue measure zero. □

This is not a lower bound for unrestricted constant positive generators. Already for $k = 1$, tilting the eigenvector of one rank-one generator can realize some interior angles with a single segment even when the signed-orbit decomposition uses two. Proposition 3.2 concerns the explicit block-efficient compiler only.

The theorem gives the complete spectrum between two familiar extremes. $q = 2\beta$ is the Pareto frontier and moves all principal planes in parallel. The profile

$$q = (2\sum_j \beta_j, 0, \dots, 0) \tag{9}$$

serializes every rotation through one instantaneous delay mode. All profiles above the Lorenz frontier interpolate exactly between parallel and serial architectures; there are no hidden continuous inequalities.

4 Rational quantization: support costs memory

The continuous theorem allows arbitrarily small nonzero angles at arbitrarily small action. A rational inner device obeys an additional integer law. Let $\zeta_0 \neq \zeta_1 \in \mathbb{T}$ and let S be an $N \times N$ rational inner matrix regular at both nodes. For a fixed rank-k input subspace $\mathcal{X}$, put $\mathcal{Y}_i = S(\zeta_i)\mathcal{X}$ and let β be the canonical-angle vector between $\mathcal{Y}_0$ and $\mathcal{Y}_1$.

Theorem 4.1 (Exact two-frequency memory quantization)**.** *Let*

$$r_\beta = \#\{j : \beta_j > 0\} = k - \dim(\mathcal{Y}_0 \cap \mathcal{Y}_1). \tag{10}$$

Then

$$\boxed{\min_S \deg_{\mathrm{McM}}(S) = r_\beta,} \tag{11}$$

where the minimum is over rational inner matrices satisfying the two subspace constraints at fixed external dimension N. Moreover, the minimizing construction can obey

$$\int_I \operatorname{tr} Q(\theta)\, \mathrm{d}\theta = 2\sum_{j=1}^{k} \beta_j \tag{12}$$

on the positively oriented arc I from ζ_0 to ζ_1 (either geometric arc may be selected by ordering the two nodes accordingly).

Proof. Let $n = \deg_{\mathrm{McM}}(S)$ and use a minimal realization

$$S(z) = D + zC(I - zA)^{-1}B, \qquad A \in \mathbb{C}^{n\times n}.$$

The resolvent identity gives

$$S(z) - S(w) = (z - w)C(I - zA)^{-1}(I - wA)^{-1}B, \tag{13}$$

so $\operatorname{rank}(S(z) - S(w)) \le n$. The kernel of $(S(\zeta_1) - S(\zeta_0))|_{\mathcal{X}}$ has dimension at least $k - n$, and every vector in that kernel has a common image in $\mathcal{Y}_0 \cap \mathcal{Y}_1$. Hence $r_\beta \le n$.

For the converse, choose principal planes for the nonzero angles. A disk automorphism b_j can be chosen with

$$b_j(\zeta_0) = 1, \qquad b_j(\zeta_1) = \mathrm{e}^{2\mathrm{i}\beta_j}; \tag{14}$$

this is the two-point transitivity of disk automorphisms on the boundary. With $H_2 = 2^{-1/2}\left[\begin{smallmatrix}1 & 1\\ 1 & -1\end{smallmatrix}\right]$, the degree-one inner block

$$R_j(z) = H_2 \operatorname{diag}(1, b_j(z)) H_2 \tag{15}$$

is the identity at ζ_0 and sends the first coordinate line at ζ_1 through angle β_j. Constant unitaries align the resulting planes with the prescribed principal vectors. The direct sum of the r_β nonconstant blocks and constant identity blocks has degree r_β.

The boundary phase of a Blaschke factor is strictly increasing. Choose the automorphism in (14) so that its unwrapped phase advance on I is $2\beta_j$. The trace of the Wigner–Smith matrix of (15) is precisely that phase derivative. Summing the blocks proves (12). $\square$

Corollary 4.2 (Topological complementarity)**.** *Every degree-minimal construction in the proof stores*

$$2\pi r_\beta - 2\sum_j \beta_j \tag{16}$$

of its total trace action outside the selected arc. In particular, if $\beta_j = \varepsilon > 0$ for all j, then

$$\deg_{\mathrm{McM}}(S) \geq k \quad \textit{while} \quad \inf \int_I \operatorname{tr} Q = 2k\varepsilon \longrightarrow 0. \tag{17}$$

This is the sharp separation between amplitude and support. The continuous Lorenz region has no discontinuity at zero, whereas rational memory jumps by one whenever a new canonical direction becomes nontrivial.

5 One noisy measurement certifies both resources

Let P_i be the projections onto $\mathcal{Y}_i$ and suppose tomography gives rank-k orthogonal projections $\widehat{P}_i$ with

$$\|\widehat{P}_i - P_i\|_{\mathrm{op}} \leq \eta_i. \tag{18}$$

Let $\widehat{s}_1 \geq \cdots \geq \widehat{s}_k$ be the k largest singular values of $(I - \widehat{P}_0)\widehat{P}_1$.

Theorem 5.1 (Fail-closed joint certificate)**.** *With $\eta = \eta_0 + \eta_1$, define*

$$\beta_j^{\mathrm{cert}} = \arcsin\bigl(\min\{1, [\widehat{s}_j - \eta]_+\}\bigr). \tag{19}$$

Then, on the event (18)*, every square rational inner S regular at the two nodes and realizing the subspace data obeys*

$$\deg_{\mathrm{McM}}(S) \geq \#\{j : \widehat{s}_j > \eta\}, \tag{20}$$

$$\int_I \sum_{j=1}^{r} \lambda_j(Q)\,\mathrm{d}\theta \geq 2\sum_{j=1}^{r} \beta_j^{\mathrm{cert}}, \qquad r = 1, \ldots, k. \tag{21}$$

Values exactly at the threshold are never counted.

Proof. Writing $A = (I - P_0)P_1$ and $\widehat{A} = (I - \widehat{P}_0)\widehat{P}_1$ gives $\|A - \widehat{A}\|_{\mathrm{op}} \leq \eta_0 + \eta_1$. The nonzero singular values of A are $\sin\beta_j$. Weyl's singular-value inequality proves $\sin\beta_j \geq [\widehat{s}_j - \eta]_+$. Apply Theorem 4.1 for (20) and the positive-delay hierarchy on the positively oriented arc I for (21). $\square$

The output is simultaneously discrete and continuous: a certified number of internal states and a certified lower Lorenz curve for the action those states must carry.

6 Proper delays are diagonal memory

The two-frequency theorem counts directions that move. More sampling points can reveal hidden state directions that no single pair or collection of local delay spectra resolves. Let $S : \mathbb{D} \to \mathbb{C}^{p\times p}$ be rational inner of degree d, regular at distinct boundary nodes $\zeta_1, \ldots, \zeta_L$. Put

$$U_i = S(\zeta_i), \qquad Q_i = -\mathrm{i}U_i^* \partial_\theta S(\mathrm{e}^{\mathrm{i}\theta})|_{\zeta_i}. \tag{22}$$

Define the $Lp \times Lp$ block matrix

$$G_{ij} = \begin{cases} \dfrac{I - U_i U_j^*}{1 - \zeta_i \bar{\zeta}_j}, & i \neq j, \\ U_i Q_i U_i^*, & i = j. \end{cases} \tag{23}$$

Theorem 6.1 (Pick–Wigner–Smith memory theorem)**.** *The finite-data matrix* (23) *satisfies*

$$G \succeq 0, \qquad \operatorname{rank} G \leq d. \tag{24}$$

For a minimal unitary realization there are matrices $F_i \in \mathbb{C}^{p\times d}$ such that

$$G_{ij} = F_i F_j^*. \tag{25}$$

Thus G is the Gram matrix of the internal states excited by the sampled frequencies and channels. Equality $\operatorname{rank} G = d$ *holds exactly when those states span the realization space.*

Proof. Every square rational inner function admits a minimal conservative unitary colligation whose state dimension is $d = \deg_{\mathrm{McM}}(S)$; regularity at the sampled boundary nodes ensures the boundary resolvents below exist. Take such a realization

$$S(z) = D + zC(I - zA)^{-1}B.$$

The lossless realization identity is

$$\frac{I - S(z)S(w)^*}{1 - z\bar{w}} = C(I - zA)^{-1}(I - \bar{w}A^*)^{-1}C^*. \tag{26}$$

Set $F_i = C(I - \zeta_i A)^{-1}$. Off the diagonal, (25) follows directly. On the boundary diagonal, the Carathéodory–Julia limit gives

$$K_S(\zeta_i, \zeta_i) = \zeta_i S'(\zeta_i)U_i^* = U_i Q_i U_i^*, \tag{27}$$

which proves the same factorization. Positivity and the rank bound are now immediate. □

The pinching inequality gives a spectral statement that local delays alone cannot reverse:

$$\lambda\left(\bigoplus_i U_i Q_i U_i^*\right) \prec \lambda(G). \tag{28}$$

Cross-frequency coherence can concentrate many nonzero local delay blocks in a much smaller hidden state space. Two convenient degree lower bounds are

$$d \geq \operatorname{rank} G \geq \frac{(\operatorname{tr} G)^2}{\operatorname{tr}(G^2)}. \tag{29}$$

Example 6.2 (Equal local delays, different hidden memory)**.** Take scalar nodes $\zeta_1 = 1$, $\zeta_2 = -1$ and

$$S_1(z) = z, \qquad S_2(z) = \left(\frac{z - \mathrm{i}/\sqrt{3}}{1 + \mathrm{i}z/\sqrt{3}}\right)^2. \tag{30}$$

The scalar proper delay of a Blaschke product is the sum of its Poisson kernels. Direct substitution gives

$$Q_1(1) = Q_1(-1) = Q_2(1) = Q_2(-1) = 1. \tag{31}$$

Nevertheless,

$$\lambda(G_1) = (2, 0), \qquad \lambda(G_2) = (1 + \sqrt{3}/2, 1 - \sqrt{3}/2). \tag{32}$$

Thus the two local delay lists are identical, while the Pick ranks recover degrees one and two exactly. The missing information is entirely in the measured scattering phases and hence in the off-diagonal blocks.

7 Robust Pick rank and reduction barriers

Suppose $\widehat{U}_i$ are unitary estimates and $\widehat{Q}_i$ are Hermitian estimates satisfying

$$\max_i \|\widehat{U}_i - U_i\|_{\mathrm{op}} \le \varepsilon_U, \qquad \max_i \|\widehat{Q}_i - Q_i\|_{\mathrm{op}} \le \varepsilon_Q, \qquad \max_i \|Q_i\|_{\mathrm{op}} \le q_{\max}. \tag{33}$$

Let

$$\delta = \min_{i \ne j} |1 - \zeta_i \bar{\zeta}_j| > 0 \tag{34}$$

and build $\widehat{G}$ from the measured data by (23).

Theorem 7.1 (Deterministic noisy-memory certificate)**.** *Define*

$$\eta_G = \varepsilon_Q + 2q_{\max}\varepsilon_U + (L-1)\frac{2\varepsilon_U}{\delta}. \tag{35}$$

Then $\|\widehat{G} - G\|_{\mathrm{op}} \le \eta_G$ *and therefore*

$$\boxed{d \ge \#\{j : \lambda_j(\widehat{G}) > \eta_G\}.} \tag{36}$$

If $\lambda_{\min}(\widehat{G}) < -\eta_G$*, no rational inner network is compatible with the stated error budget.*

Proof. For diagonal blocks, unitary invariance and (33) give

$$\|\widehat{U}_i \widehat{Q}_i \widehat{U}_i^* - U_i Q_i U_i^*\|_{\mathrm{op}} \le \varepsilon_Q + 2q_{\max}\varepsilon_U.$$

For $i \ne j$, the corresponding bound is $2\varepsilon_U / |1 - \zeta_i \bar{\zeta}_j|$. The block row-sum bound proves (35); Weyl's theorem and Theorem 6.1 prove (36) and the falsifier. □

Corollary 7.2 (Unavoidable reduction tails)**.** *Let G be the exact memory Gram matrix of a device. Every degree-r rational inner approximant, with corresponding sample matrix $\widetilde{G}$, satisfies*

$$\|G - \widetilde{G}\|_{\mathrm{op}} \ge \lambda_{r+1}(G), \tag{37}$$

$$\|G - \widetilde{G}\|_F \ge \left(\sum_{j>r} \lambda_j(G)^2 \right)^{1/2}. \tag{38}$$

More generally, every unitarily invariant norm is bounded below by the matching spectral tail.

Proof. $\operatorname{rank} \widetilde{G} \le r$ by Theorem 6.1; apply the Eckart–Young–Mirsky theorem. □

This is a model-reduction obstruction in measured coordinates, not an asymptotic statement about a chosen identification algorithm.

8 A transfer-matrix corollary

The positive-kernel viewpoint also gives a precise bridge to transfer matrices. Let $0 < T < I$ be a finite-dimensional positive self-adjoint contraction and define

$$S_T(z) = (zI - T)(I - zT)^{-1}. \tag{39}$$

This self-adjoint Schur-to-inner transform is classical [1]; we record its consequence for delay and Euclidean correlators.

Proposition 8.1 (Transfer–delay dictionary). *The function* (39) *is inner and*

$$Q_T(\theta) = \big(I - T^2\big)\big(I - 2T\cos\theta + T^2\big)^{-1}, \tag{40}$$

$$= I + 2\sum_{n\geq 1} T^n \cos(n\theta). \tag{41}$$

Hence, for any observable map V, the Euclidean correlators $C_n = V^*T^nV$ are exactly the complex Fourier coefficients of $V^*Q_T(\theta)V$ (equivalently, the coefficients in its cosine expansion (41)*). If $T = \mathrm{e}^{-H}$ on a vacuum-orthogonal sector, then*

$$Q_T(0) = \coth(H/2), \qquad H \succeq mI \iff Q_T(0) \preceq \coth(m/2)I. \tag{42}$$

Proof. Diagonalize T and apply the scalar Blaschke and Poisson-kernel identities to each eigenvalue. Equation (42) follows by functional calculus and monotonicity of $t \mapsto (1+t)/(1-t)$. □

For the $SU(2)$ heat semigroup used in two-dimensional Yang–Mills, the non-vacuum class-function eigenvalues are $\exp[-an(n+2)/4]$, $n \geq 1$. Therefore

$$h_n = \frac{an(n+2)}{4}, \qquad q_n(0) = \coth\left(\frac{an(n+2)}{8}\right), \qquad \|Q(0)\|_{\mathrm{op}} = \coth(3a/8). \tag{43}$$

The semigroup and its $SU(2)$ spectrum are independently formalized in the companion Lean development [9].

Limitation 8.2 (Dictionary, not a mass-gap proof). Equation (42) reparametrizes a known transfer spectrum; it does not establish a gap for an interacting theory. The vacuum eigenvalue $T = 1$ must be projected out. A compression V^*Q_TV sees only the cyclic sector generated by V and can miss a slower orthogonal mode exactly. Infinite-dimensional field theories also lie outside the rational finite-degree statements of Theorems 4.1 and 6.1.

This restricted corollary is included because it gives a falsifiable bridge between the passive-network resource and Euclidean data without claiming a solution of the Yang–Mills mass-gap problem.

9 Reproducible adversarial audit

All principal results are analytic. The computational artifact attacks the constructive and finite-precision interfaces:

1. a flagship rank-three profile with four compiler segments, positive Lorenz margins, endpoint error 4.5×10^{-16} and commutator norm below 10^{-16};
2. 192 random feasible profiles of ranks one through four, each solved by linear programming over its signed permutahedron and reconstructed by exact matrix exponentials; the worst endpoint/profile error is below 4.5×10^{-14} and no compiler uses more than $k+1$ segments;
3. 256 random two-node Blaschke compilers, verifying endpoint phases, principal angles, positive delay and the sharp integrated arc action;
4. 512 noisy rank-k projector pairs, with no degree overcount and no violation of any certified Lorenz prefix;
5. the exact degree-one/degree-two blindness example (30)–(32);
6. 768 random matrix Blaschke–Potapov networks, with no Pick-rank violation and 743 generic full-degree recoveries;
7. 512 noisy matrix instances, with no robust rank overcount and a largest actual-error/bound ratio below 0.476; and

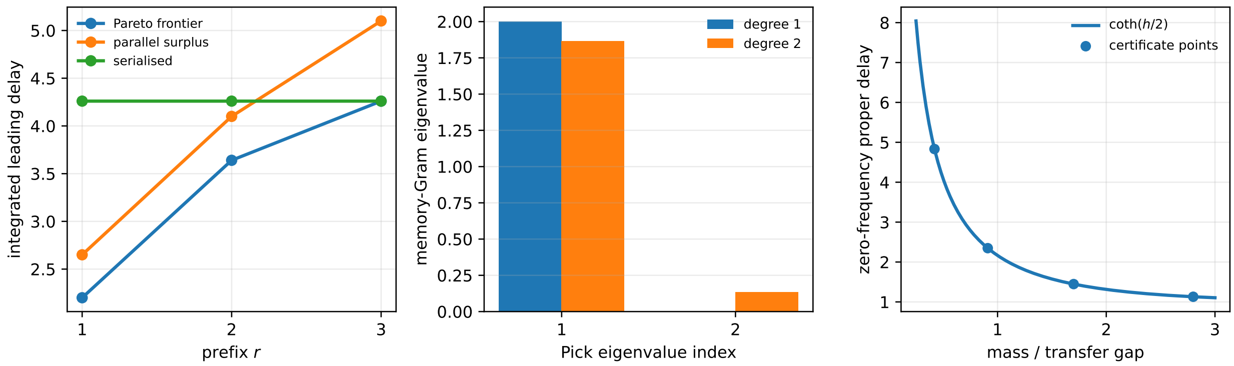

Figure 1: Left: the complete Lorenz region contains parallel, surplus and serial resource allocations. Centre: two scalar networks have identical local proper delays at both nodes, but Pick spectra of ranks one and two. Right: the transfer gap and zero-frequency delay are related exactly by $q = \coth(h/2)$.

8. the transfer identity on 8,192 Fourier nodes, recovering four coefficients with error below 2.6×10^{-15}.

An independent verifier rebuilds the compiler from the frozen signed vertices, checks positivity, commutativity, endpoint angles and exact delay profile, rederives the strict example, and runs separately coded scalar and matrix Pick, noisy-projector, noisy-rank and Blaschke-action probes. The JSON certificate, figure, source and release manifest are hash-locked and replayed in continuous integration.

10 Scope, falsifiers and open problems

Limitation 10.1 (Continuous synthesis is not rational synthesis). The compiler in Theorem 3.1 is an absolutely continuous unitary path with piecewise-constant positive generator. It need not be the boundary trace of a rational inner function of a prescribed degree. The quantization theorem solves exactly the two-node subspace problem, not arbitrary profile interpolation on a whole arc.

Limitation 10.2 (Subspaces, not calibrated frames). The degree r_β is exact for subspace constraints. Prescribing phases or complete frames can require additional degree. Conversely, allowing hidden loss ports requires a unitary dilation before any inner or Wigner–Smith rank claim is applied.

Limitation 10.3 (Node separation is a resource). The robust Pick threshold deteriorates as $\delta = \min_{i \neq j} |1 - \zeta_i \bar{\zeta}_j|$ tends to zero. Closely spaced samples require derivative data of higher accuracy or a confluent Pick formulation. A substantially negative eigenvalue beyond (35) falsifies the claimed lossless passive model.

Three questions now have precise targets: characterize the rational-inner subset of the full Lorenz region at fixed degree; derive a confluent robust kernel for clustered frequency samples; and determine when small Pick tails imply an operator-norm-nearby passive reduced model, rather than only the necessary lower bounds (37)–(38).

11 Conclusion

Passive subspace transport has a complete continuous resource region: $2\beta \prec_w q$ is necessary and sufficient, and every feasible point is compiled by at most $k+1$ commuting positive segments with constant proper-delay spectrum. Rationality then quantizes a transverse resource: the minimum memory degree is the number of nonzero canonical angles. One noisy projector spectrum certifies both the integer support cost and the continuous Lorenz cost.

Across multiple frequencies, proper delays are only diagonal memory. The boundary Pick matrix restores the missing cross-frequency coherences, is literally a Gram matrix of internal states, and yields robust rank and model-reduction obstructions. The strict degree-one/degree-two example proves that this information is operationally new. The resulting picture is a two-layer resource theory: majorization controls how much motion is required, while analytic rank controls how many hidden states must exist to realize it.

Data and code availability

The final manuscript, generator, independent verifier, frozen JSON certificate, figure and hash manifest are archived in the immutable GitHub release v1.7 of the companion repository. Theorems are proved analytically in the text; numerical tests are adversarial audits and do not substitute for the proofs.

References

[1] Yu. M. Arlinskiĭ and Seppo Hassi. Holomorphic operator-valued functions generated by passive selfadjoint systems. *Methods of Functional Analysis and Topology*, 24(2):101–127, 2018.

[2] Joseph A. Ball and Jeongook Kim. Stability and McMillan degree for rational matrix interpolants. *Linear Algebra and its Applications*, 196:207–232, 1994.

[3] Vladimir Bolotnikov and Harry Dym. *On Boundary Interpolation for Matrix Valued Schur Functions*, volume 181, no. 856 of *Memoirs of the American Mathematical Society*. American Mathematical Society, 2006.

[4] Louis de Branges and James Rovnyak. *Square Summable Power Series*. Holt, Rinehart and Winston, New York, 1966.

[5] Lluis Eriksson. Architecture-dependent decoherence suppression in passive quantum networks. GitHub release, 2026. Immutable artifact.

[6] Lluis Eriksson. Every spectral switch costs memory. GitHub release, 2026. Immutable artifact.

[7] Lluis Eriksson. Finite-sample spectral-edge exclusion. GitHub repository, 2026. Reproducible repository.

[8] Lluis Eriksson. Irreducible channel mixing and exponential calibration laws. GitHub release, 2026. Immutable artifact.

[9] Lluis Eriksson. Lean formalization of two-dimensional Yang–Mills heat semigroups. GitHub repository, 2026. Formalization repository.

[10] Lluis Eriksson. Lossless calibration is stored memory. GitHub release, 2026. Immutable artifact.

[11] Lluis Eriksson. Proper-delay spectra majorize subspace rotation: Exact finsler resource laws for passive networks. GitHub release, 2026. Immutable artifact.

[12] A. E. Frazho, A. C. M. Ran, and F. van Schagen. Finite dimensional Naimark realizations and choice sequences. *Integral Equations and Operator Theory*, 98(2):1–25, 2026.

[13] John E. Gough and Guofeng Zhang. On realization theory of quantum linear systems. *Automatica*, 59:139–151, 2015.

[14] Shin-Ming Huang. Quantum-state projectors on Grassmannian: Geometry, holonomy, and topology, 2026. Preprint, 7 August 2026.

[15] Albert W. Marshall, Ingram Olkin, and Barry C. Arnold. *Inequalities: Theory of Majorization and Its Applications*. Springer, New York, 2 edition, 2011.

[16] Pedro Massey, Demetrio Stojanoff, and Sebastián Zárate. The spectral spread of hermitian matrices. *Linear Algebra and its Applications*, 616:19–44, 2021.

[17] Brockway McMillan. Introduction to formal realizability theory—i. *Bell System Technical Journal*, 31(2):217–279, 1952.

[18] Li Qiu, Yanxia Zhang, and Chi-Kwong Li. Unitarily invariant metrics on the Grassmann space. *SIAM Journal on Matrix Analysis and Applications*, 27(2):507–531, 2005.